Supplementary Information

Origin of Capacity Rising in $LiFePO_4$ Batteries: Practical Implications for Reliable Cell Design

Minsoo Kim,[*a] Jinsu Ha,[a] Moon-Seok Kwon,[a] Bokhyun Ka,[a] Sanghee Nam,[b] Sunyhik Ahn,[c] Soonsung Suh,[d] Songyul Oh[d] and Ayoung Kim[d]

[a]Cell Diagnosis Lab., Electrode Development Team, Samsung SDI, Suwon, 16678, Republic of Korea

[b]Platform Electrode Group, Electrode Development Team, Samsung SDI, Suwon, 16678, Republic of Korea

[c]Advanced Electrode Group, Electrode Development Team, Samsung SDI, Suwon, 16678, Republic of Korea

[d]Cell Development Group 3, Automotive & ESS Battery Business, Samsung SDI, Yongin, 16678, Republic of Korea

Corresponding author: Minsoo Kim; soo75.kim@samsung.com

EXPERIMENTAL METHODS

Three-electrode tests

Three-electrode tests were carried out using a commercial cell (EL-CELL, PAT-Cell). LFP ($LiFePO_4$) cathodes, graphite (Gr) anodes, and glass fiber separators were punched to a diameter of 18 mm. A sparse stainless steel mesh was used as the reference electrode and was sandwiched between two separators. The electrolyte consisted of $LiPF_6$ salt dissolved in a carbonate-based solvent. After assembling the three-electrode cell in a dry room, Li metal was plated onto the reference electrode by applying a current of 10 μA for 5 hours. The cell was then charged and discharged at 0.05C between 2.5 V and 3.65 V for formation. Electrochemical impedance spectroscopy (EIS) was performed at SOC50 before and after nine charge-discharge cycles at 0.5C/1C. EIS measurements were conducted over a frequency range of 1 MHz to 1 mHz with a sinusoidal amplitude of 10 mV.

Voltage profile matching of anode and cathode in dV/dQ profiles

Cathode and anode half-cells were fabricated using the same electrodes as those used in the full cell. After formation, the half-cells were charged at 0.05C and discharged at 1C. The voltage range was set from 3 V to 3.7 V for the cathode and from 0.01 V to 1.5 V for the anode. Full cells were also charged at 0.05C to 3.65 V and discharged at 1C to 2.5 V at 0, 120, and 480 cycles for matching the dV/dQ profiles.

The differential voltage profile of the anode half-cell during charge was aligned with that of the full cell, enabling precise matching due to the characteristic staging behavior of Gr. The voltage profile (not the differential voltage) of the cathode half-cell during discharge was aligned with both ends of the full-cell voltage profile. This approach was feasible because the charge process was always limited by the steep slope of the LFP cathode, and the discharge

process was also determined by the cathode, as the 1C rate was sufficiently fast to induce cathode-limited discharge, as shown in Fig. S15.

Cell fabrication and cycle tests

LFP and Gr were used as the cathode and anode materials, respectively. LFO (Li_5FeO_4) was added at 1% or 2% as a sacrificial cathode additive. $LiPF_6$ salt dissolved in a carbonate solvent was used as the electrolyte, and a PE separator was employed. The cathode and anode electrodes were stacked and assembled into prismatic cells in a dry room. All cells were charged to 3.65 V at 0.5C with a 0.2C cut-off in constant voltage (CV) mode, then discharged to 2.5 V at 1C. A reference performance test (RPT) was conducted every 60 cycles. For the RPT, cells were charged to 3.65 V at 0.33C with a 0.02C cut-off in CV mode and discharged to 2.5 V at 0.33C. In Fig. 3e–g, to compare the effect of different C-rates, cells were cycled at 2C/0.5C and 0.5C/1C (charge/discharge) while RPTs were performed under the same conditions as for the other cells.

Calculation of cell specifications

In Fig. 4g, the gravimetric energy density was calculated based only on the weight (g) of the cathode and anode active materials, excluding other cell components. The energy (Wh) was determined by multiplying the discharge capacity by the average discharge voltage. In Fig. 4g and h, the “2% LFO (cal.)” condition simulated a cell designed to have the same uncharged anode capacity as the 0% LFO cell. The additional weight of the Gr anode, corresponding to the increased uncharged anode capacity, was included in the energy density calculation.

Quantification of the loss of lithium inventory (LLI)

When reversible Li ions are consumed, electrode slippage appears in the voltage profiles.[S1] Because the charge direction corresponds to a leftward shift in our capacity coordinate, Li loss

results in a leftward shift of the anode profile. In addition, the LFP cathode is always fully delithiated at full charge because of its steep voltage rise near the upper cutoff voltage. Therefore, at the full-charge state, LLI was quantified by measuring the shift of the anode-derived peak relative to its initial position in the full-cell voltage profile. For easier comparison, Figs. S17 and S18 show the data after alignment of the anode-derived peaks, such that the shift in the full-charge position can be directly compared.[S2]

Training and evaluation of prediction model

The ElasticNetCV module in Python was used to identify the optimal hyperparameters, including the L1 ratio and alpha. A 5-fold cross-validation was performed to train and test the elastic net regression model, and this process was randomly repeated 100 times. To evaluate the combinations of features, the average R^2 score was calculated for each feature set, and the best R^2 score was recorded for each feature count. For training and testing the prediction model, all predicted rising capacity values (7,900 data points) were recorded at each test iteration and compared with the observed rising capacity values, yielding the average R^2 and RMSE.

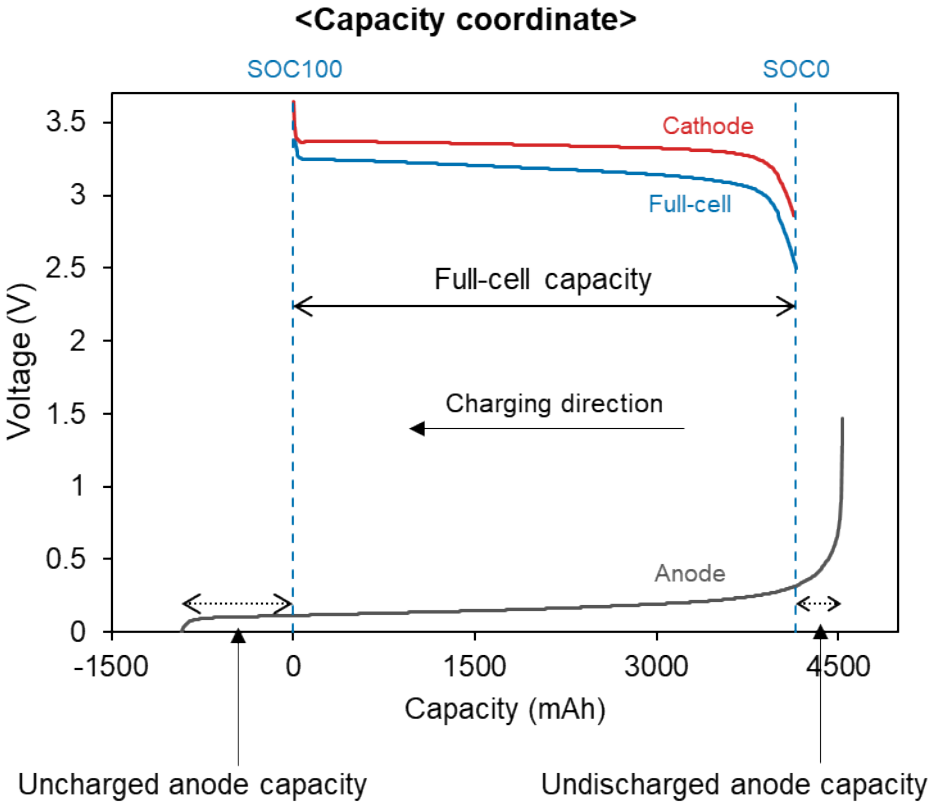

Fig. S1. Voltage profiles of cathode, anode, and full-cell aligned on capacity coordinate for an LFP/Gr full-cell at BOL.

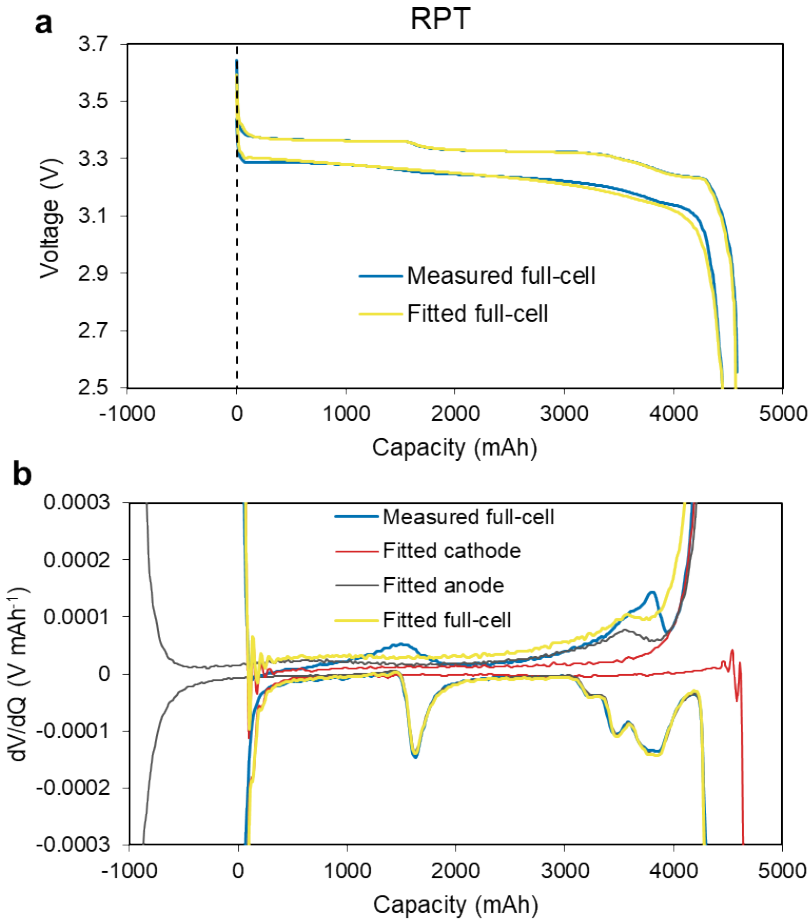

Fig. S2. (a) Measured and fitted voltage profiles, and (b) the corresponding dV/dQ profiles of measured full-cell and fitted cathode, anode, and full-cell during charge and discharge for the LFP/Gr cell at BOL for RPT.

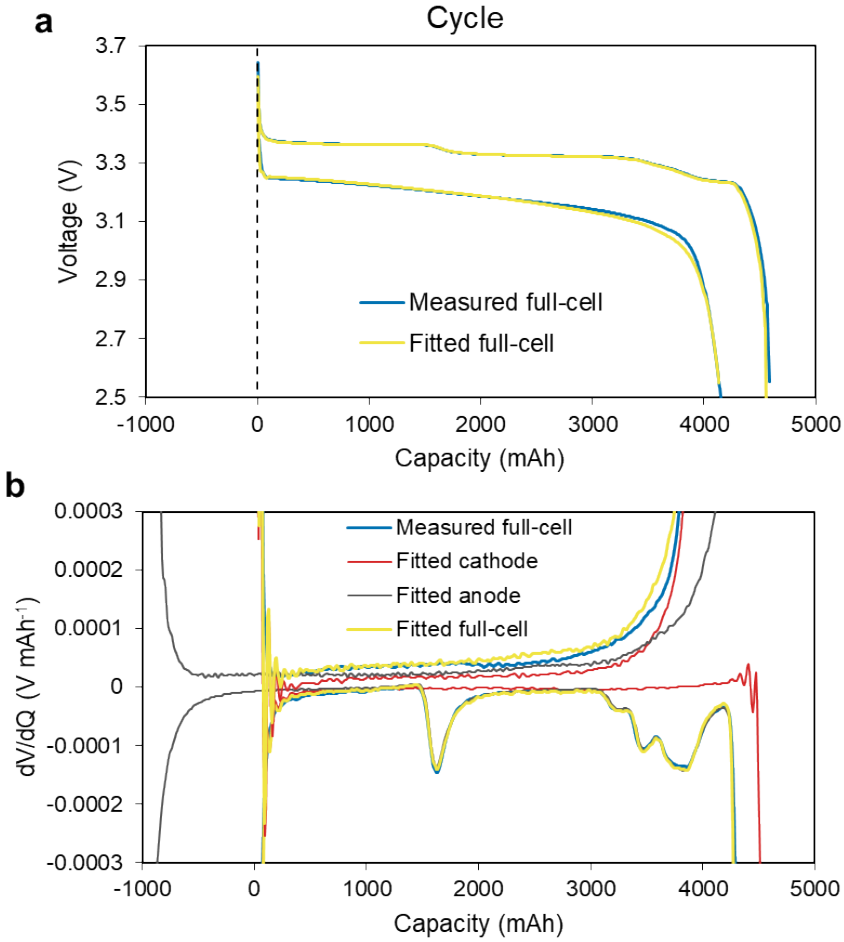

Fig. S3. (a) Measured and fitted voltage profiles, and (b) the corresponding dV/dQ profiles of measured full-cell and fitted cathode, anode, and full-cell during charge and discharge for the LFP/Gr cell at BOL for Cycle.

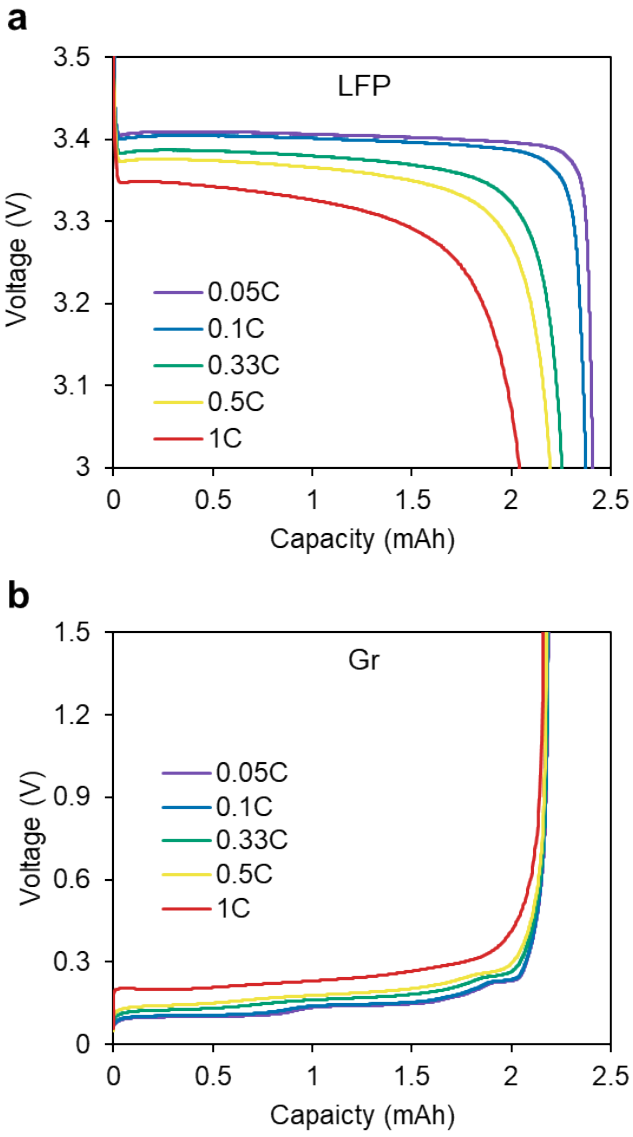

Fig. S4. Discharge voltage profiles at different discharge C-rates for (a) LFP and (b) Gr half-cells. Charge C-rate was fixed at 0.05C for every cycle.

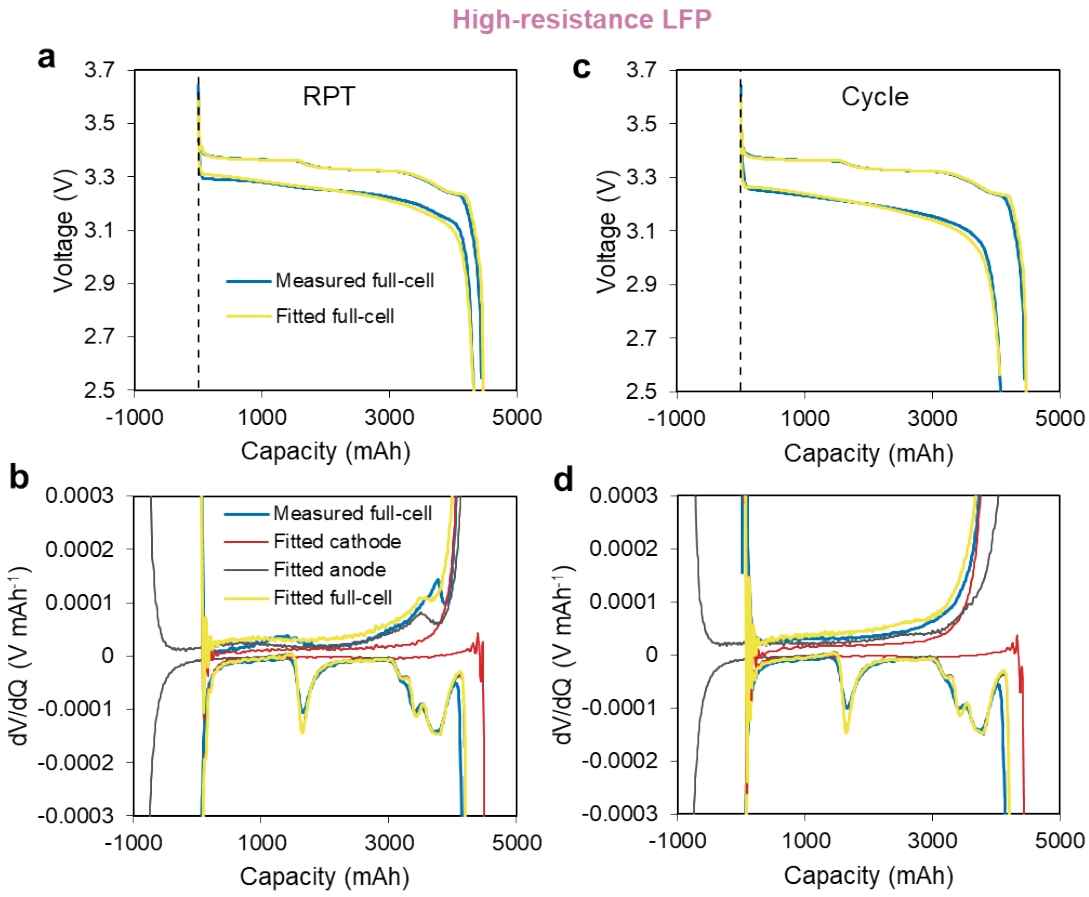

Fig. S5. (a, c) Measured and fitted voltage profiles and (b, d) the corresponding dV/dQ profiles of the measured full-cell and the fitted cathode, anode, and full-cell during charge and discharge for the LFP/Gr cell using the high-resistance LFP at BOL for RPT and Cycle, respectively.

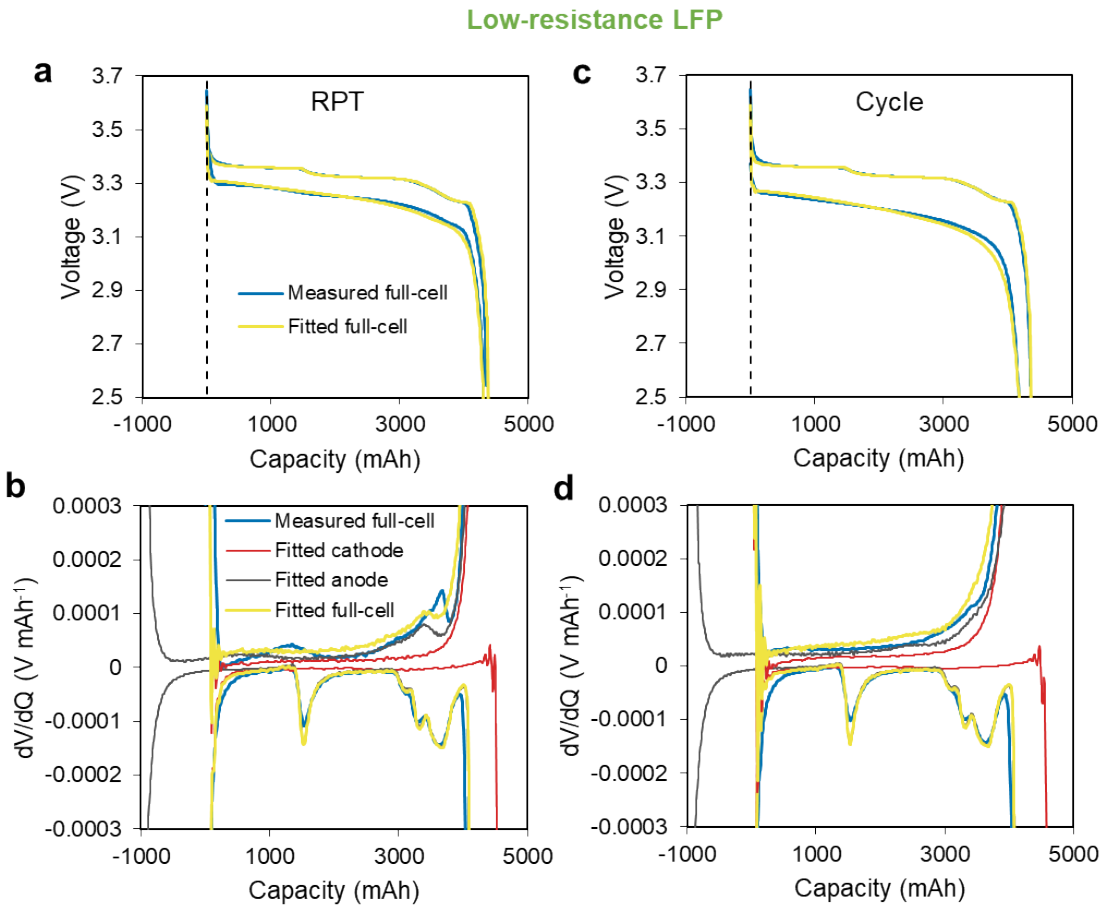

Fig. S6. (a, c) Measured and fitted voltage profiles and (b, d) the corresponding dV/dQ profiles of the measured full-cell and the fitted cathode, anode, and full-cell during charge and discharge for the LFP/Gr cell using the low-resistance LFP at BOL for RPT and Cycle, respectively.

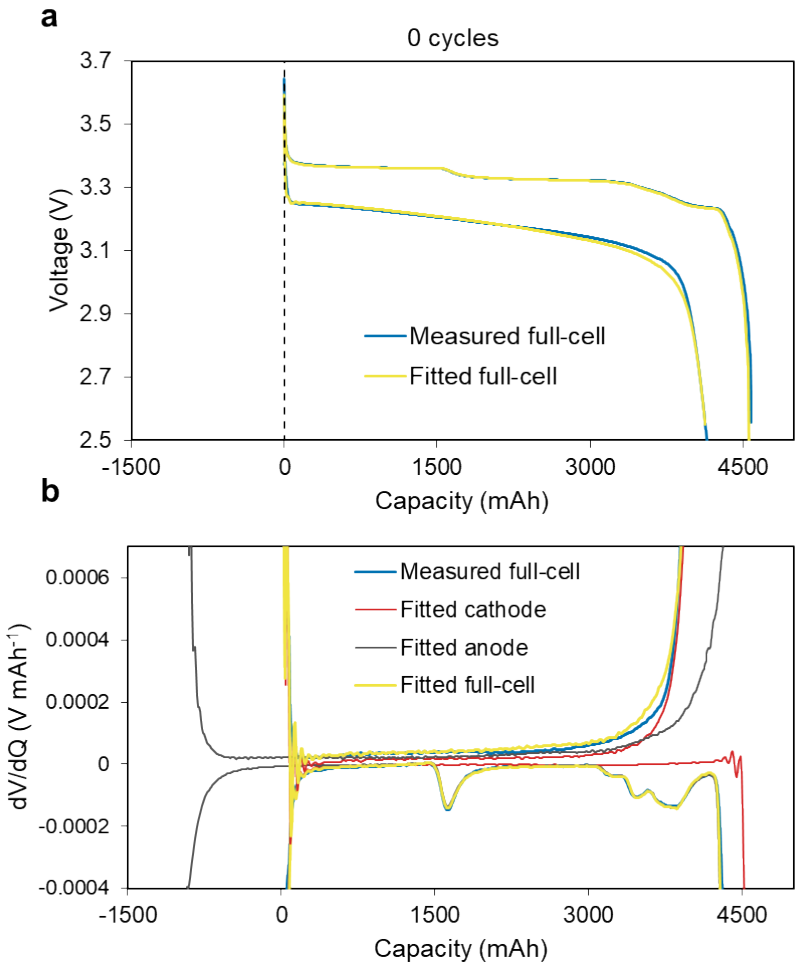

Fig. S7. (a) Measured and fitted voltage profiles, and (b) the corresponding dV/dQ profiles of measured full-cell and fitted cathode, anode, and full-cell during charge and discharge for the LFP/Gr cell at 0 cycles.

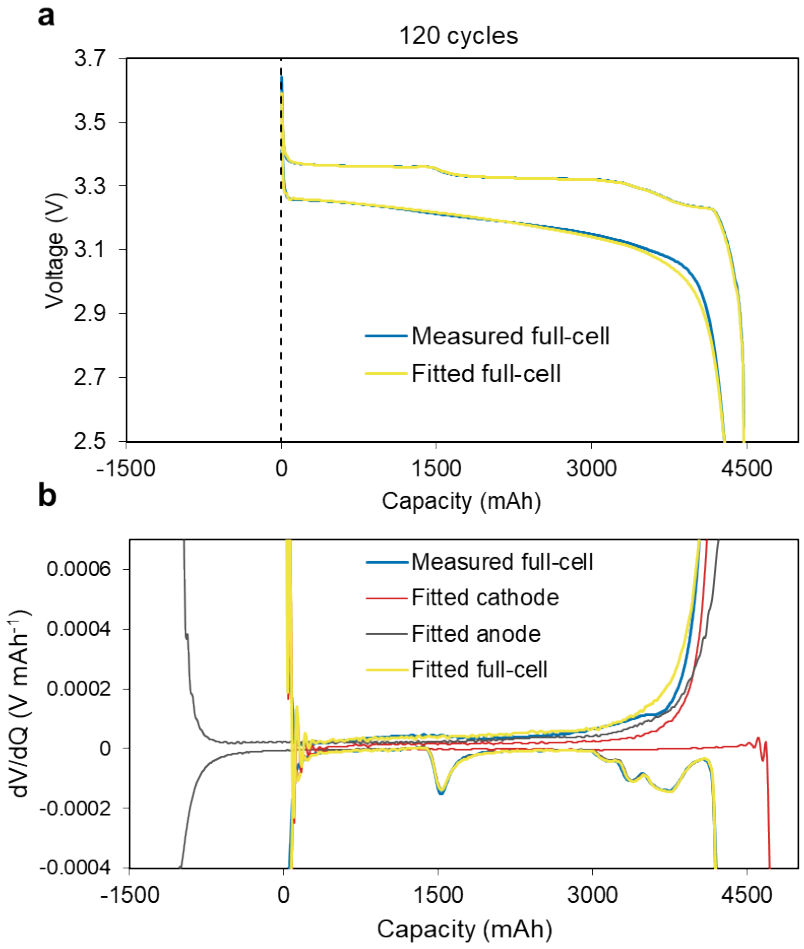

Fig. S8. (a) Measured and fitted voltage profiles, and (b) the corresponding dV/dQ profiles of measured full-cell and fitted cathode, anode, and full-cell during charge and discharge for the LFP/Gr cell at 120 cycles.

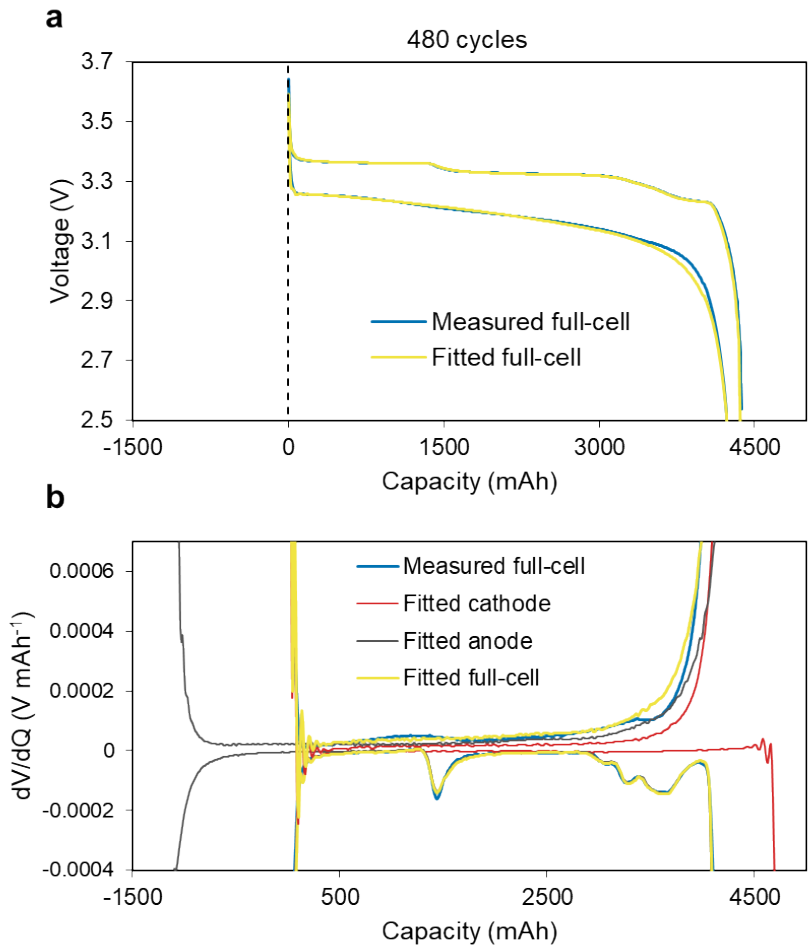

Fig. S9. (a) Measured and fitted voltage profiles, and (b) the corresponding dV/dQ profiles of measured full-cell and fitted cathode, anode, and full-cell during charge and discharge for the LFP/Gr cell at 480 cycles.

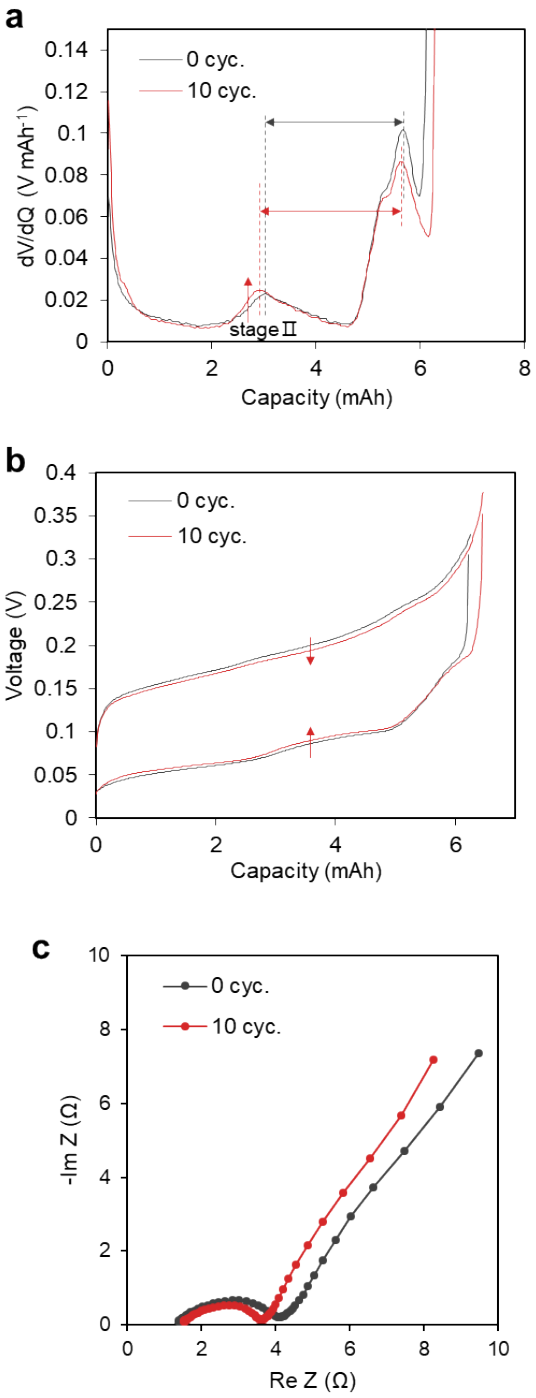

Fig. S10. (a) dV/dQ profiles during charge, (b) voltage profiles during charge and discharge, and (c) Nyquist plots for the anode of the LFP/Gr full-cell in three-electrode tests at 0 and 10 cycles.

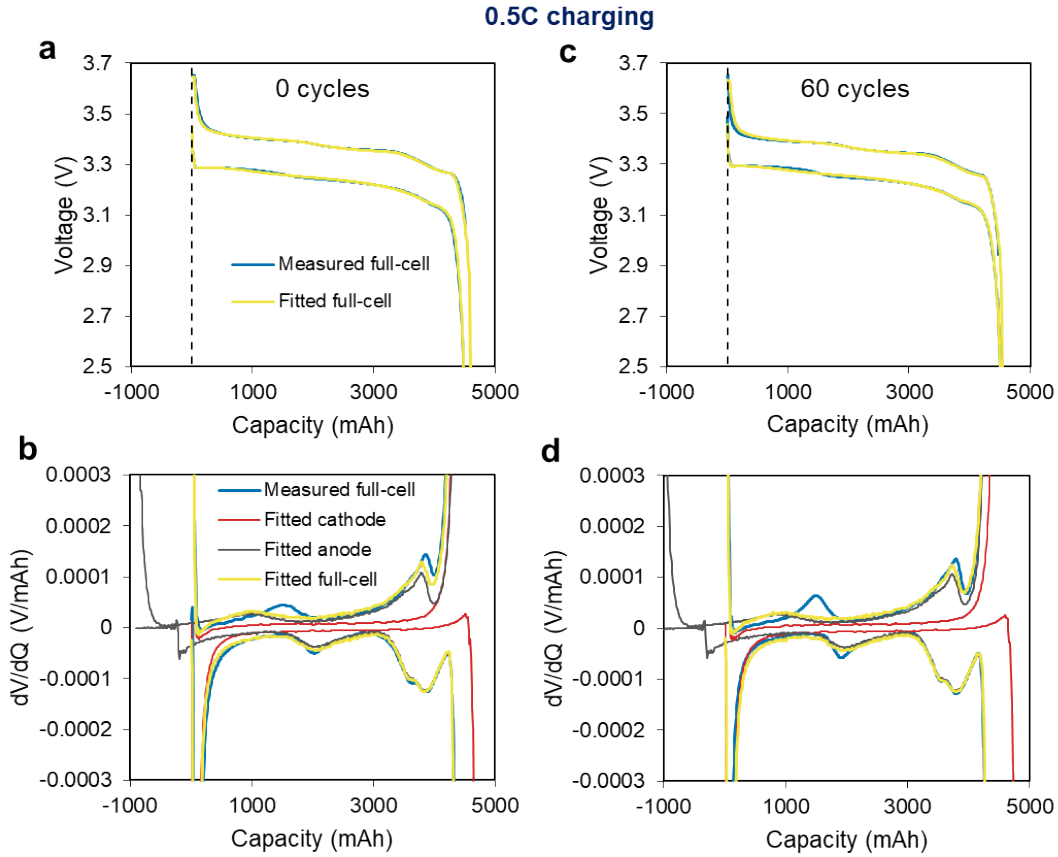

Fig. S11. (a, c) Measured and fitted voltage profiles and (b, d) the corresponding dV/dQ profiles of the measured full-cell and the fitted cathode, anode, and full-cell during charge and discharge for the LFP/Gr cell before and after 60 cycles at 0.5C charging, respectively.

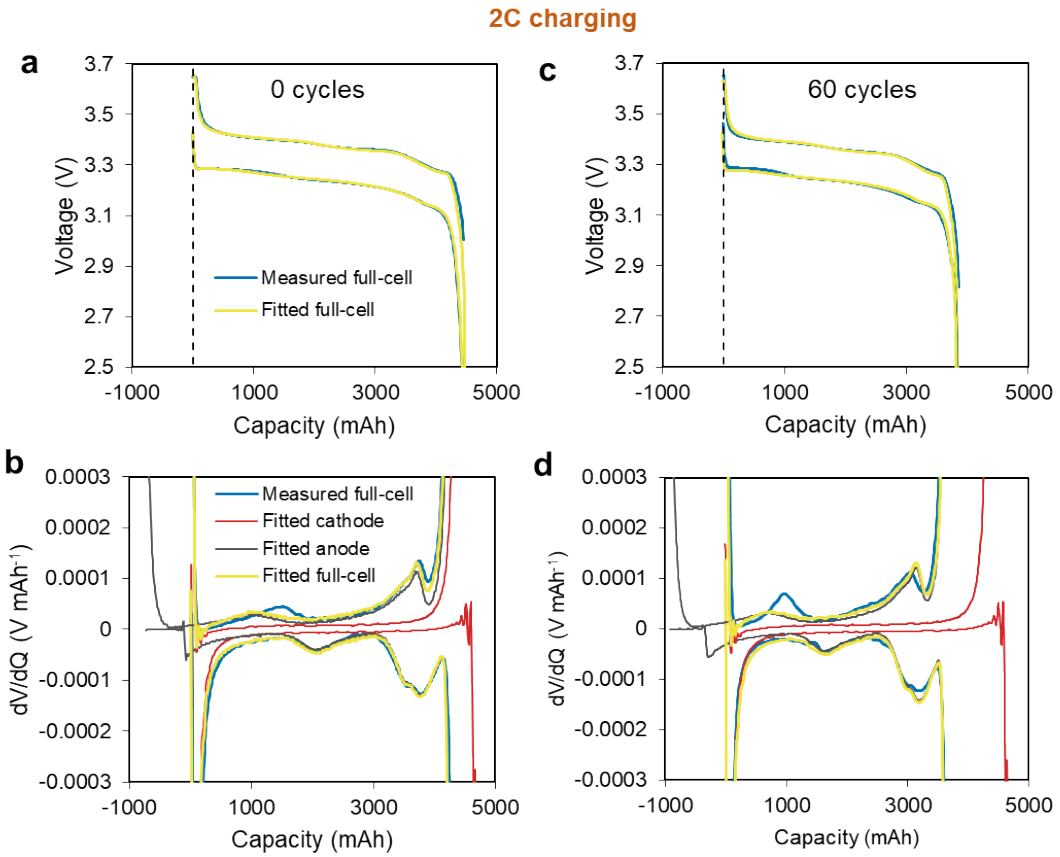

Fig. S12. (a, c) Measured and fitted voltage profiles and (b, d) the corresponding dV/dQ profiles of the measured full-cell and the fitted cathode, anode, and full-cell during charge and discharge for the LFP/Gr cell before and after 60 cycles at 2C charging, respectively.

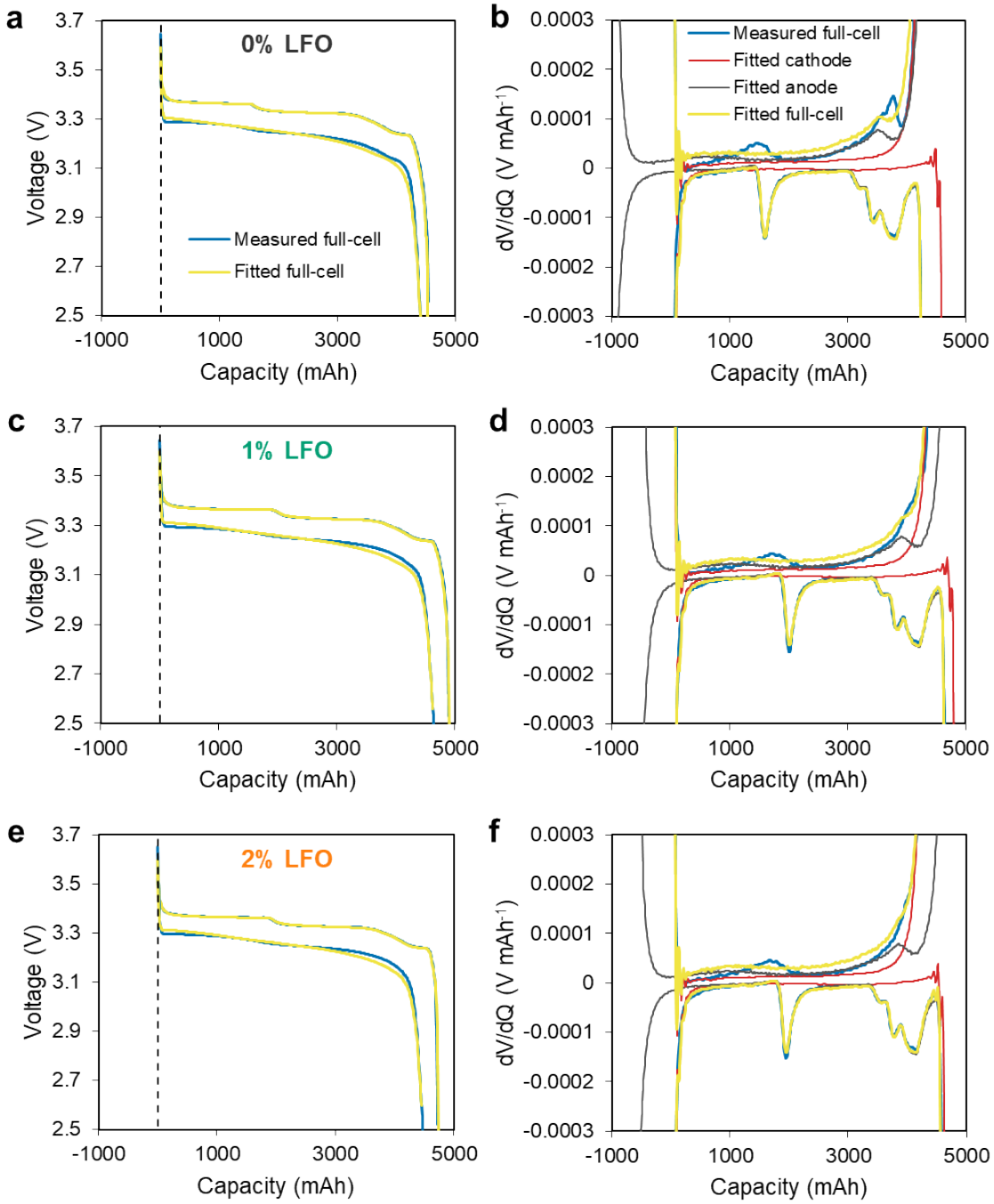

Fig. S13. (a,c,e) Measured and fitted voltage profiles and (b,d,f) the corresponding dV/dQ profiles of the measured full-cell and the fitted cathode, anode, and full-cell during charge and discharge for the LFP/Gr cells with 0%, 1%, and 2% LFO, respectively.

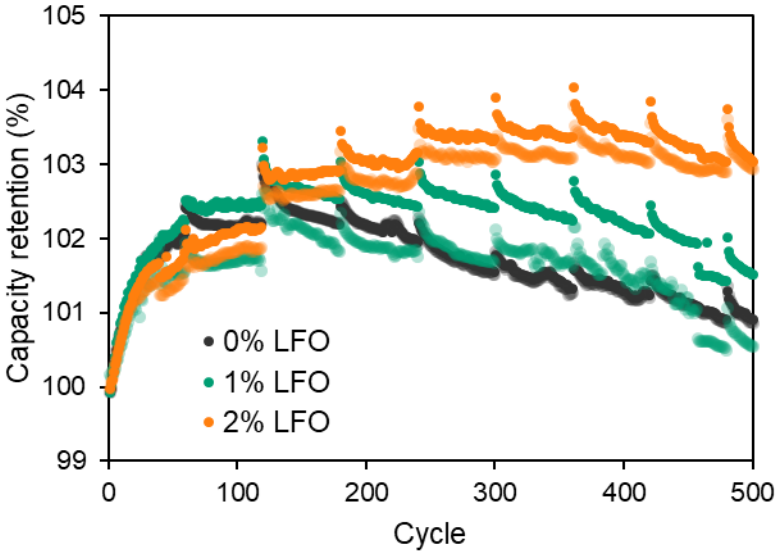

Fig. S14. Cycle retention of LFP/Gr full-cells with 0%, 1%, and 2% LFO at 0.5C/1C.

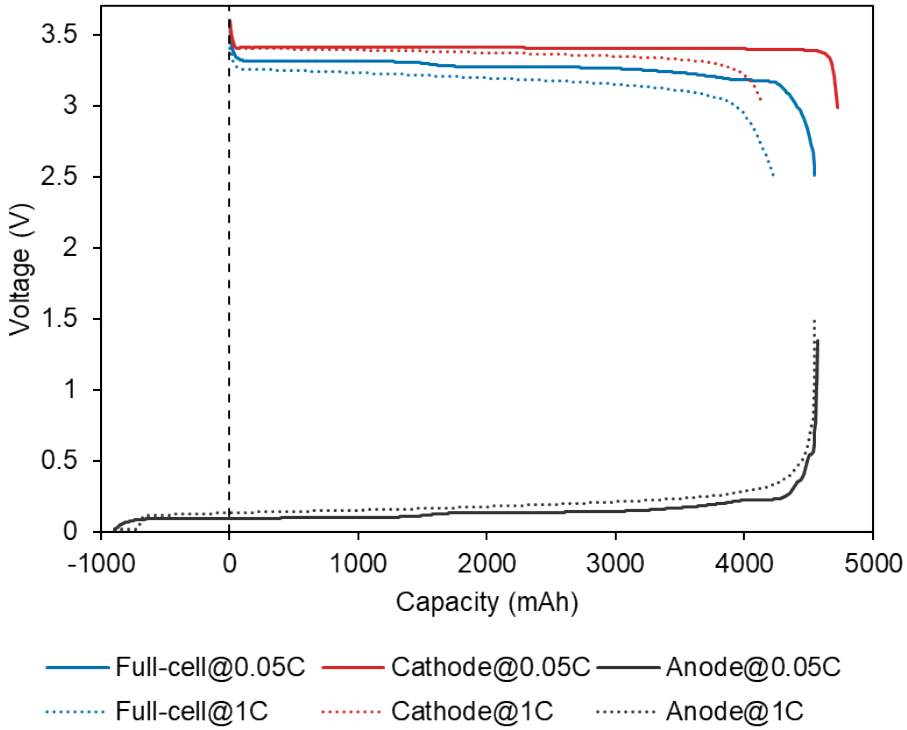

Fig. S15. Discharge voltage profiles for anode, cathode, and full-cell at 0.05C and 1C on the capacity coordinate. The cathode capacity was affected by different discharge C-rates whereas the anode capacity remained nearly constant.

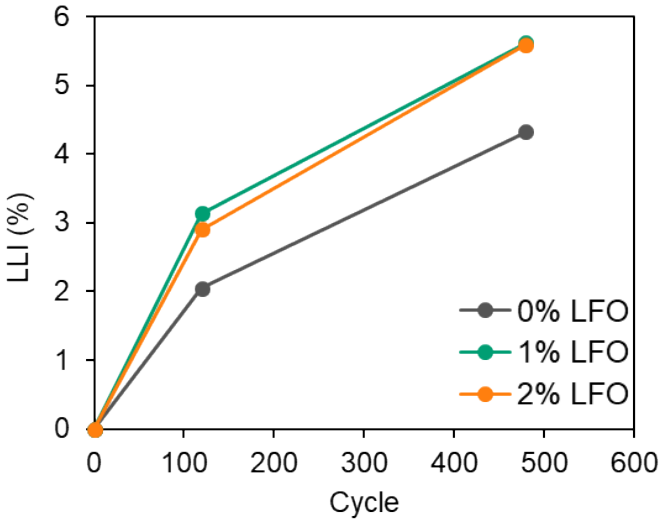

Fig. S16. LLI in LFP/Gr cells with 0%, 1%, and 2% LFO during cycling. The irreversible Li loss was calculated by dV/dQ analysis.

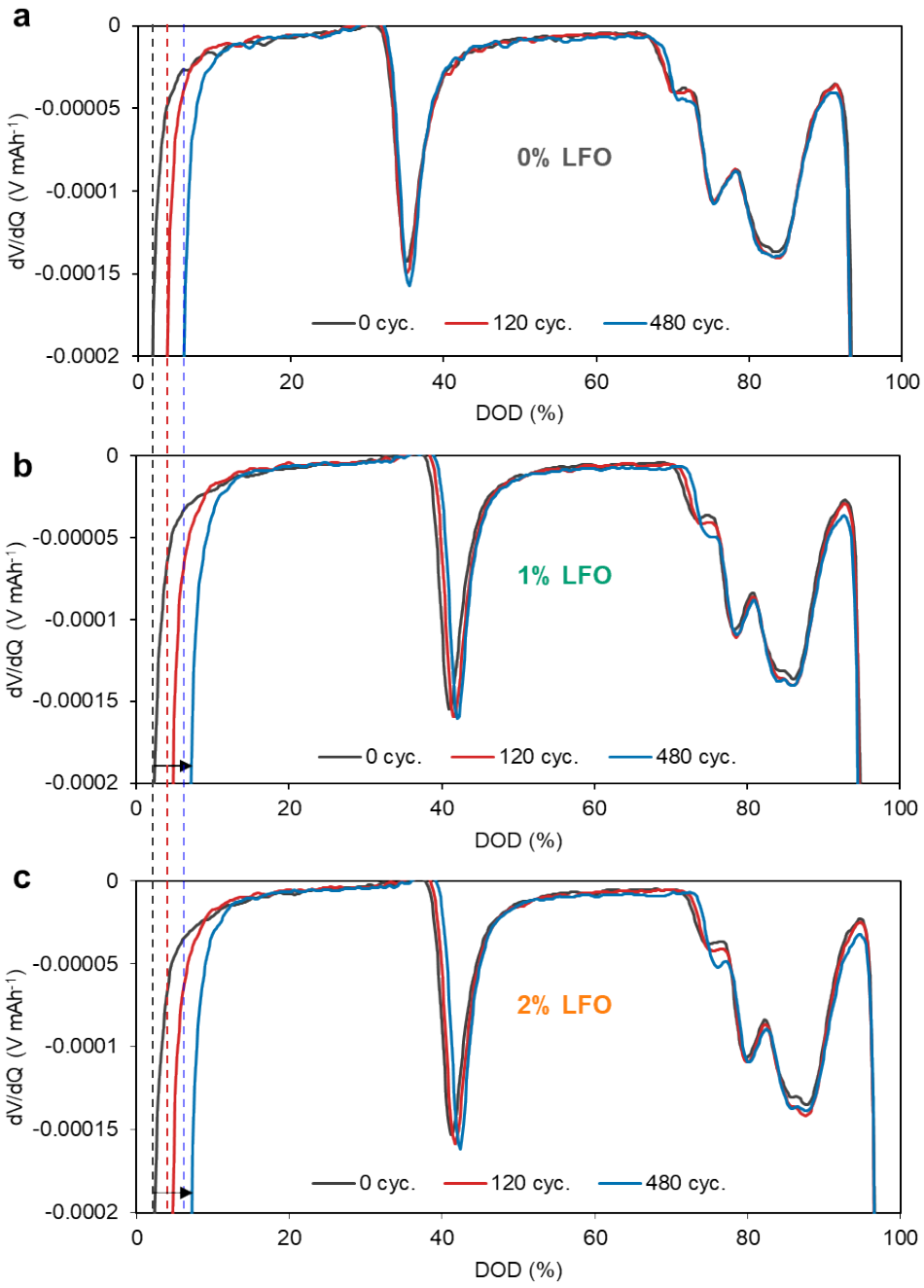

Fig. S17. Comparison of LLI with different LFO additions. dV/dQ profiles of full-cells with (a) 0%, (b) 1%, and (c) 2% LFO at 0, 120, and 480 cycles. Profiles were shifted to align the Gr stage IV peak.

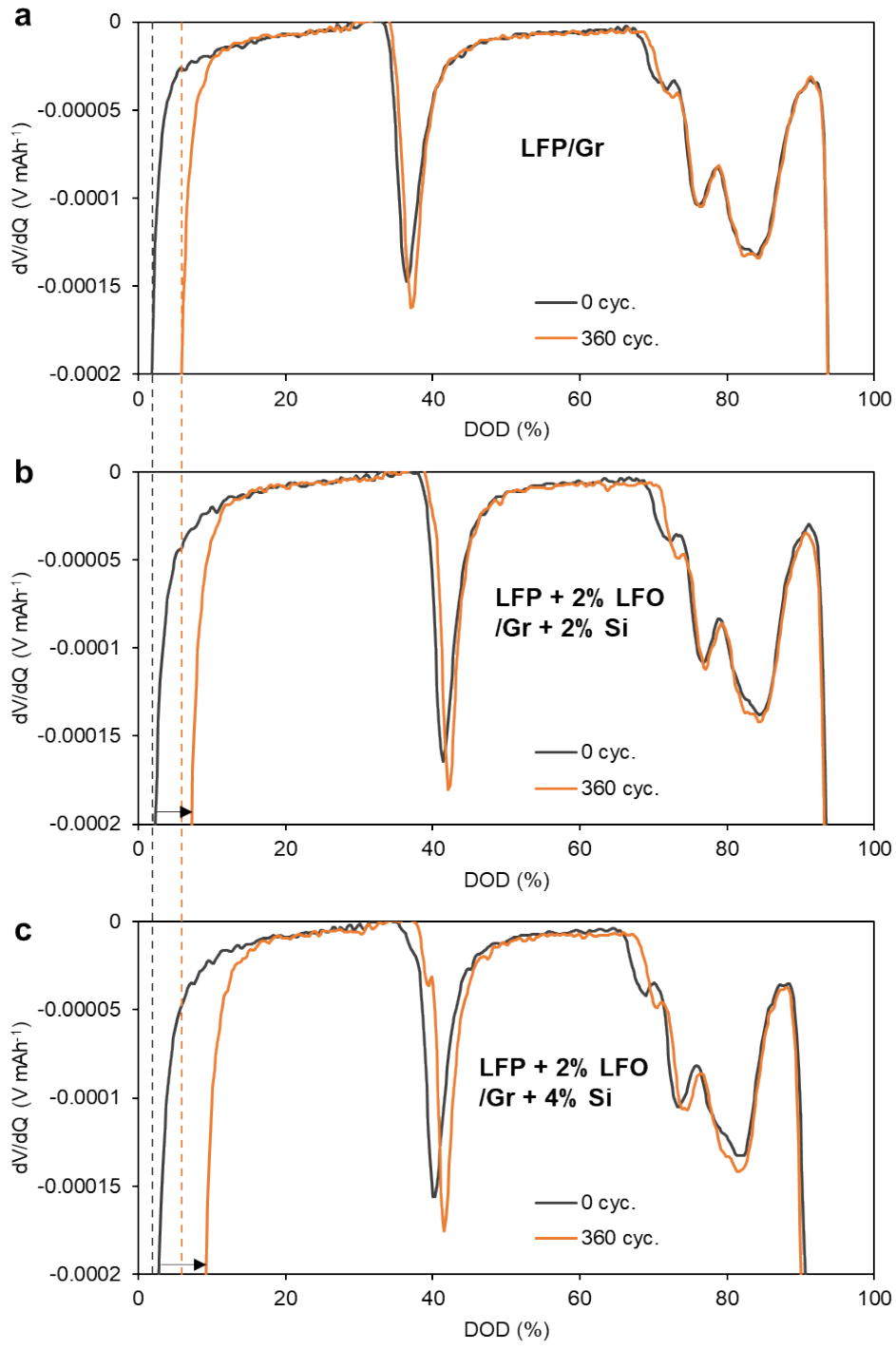

Fig. S18. Comparison of LLI with different Si additions. dV/dQ profiles of full-cells with (a) 0%, (b) 2%, and (c) 4% Si at 0 and 360 cycles. Profiles were shifted to align the Gr stage IV peak.

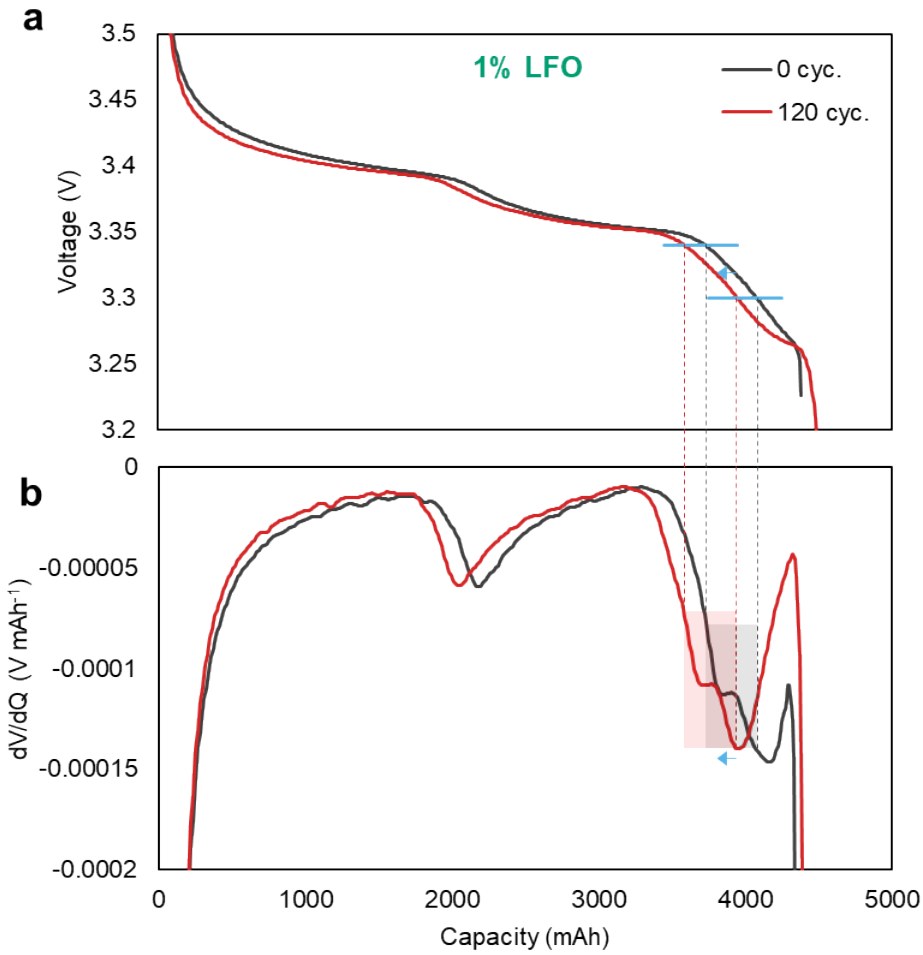

Fig. S19. Feature representing LLI. (a) Charge voltage profiles of a full-cell with LFP + 1% LFO/Gr at 0 and 120 cycles, and (b) the corresponding dV/dQ profiles.

a

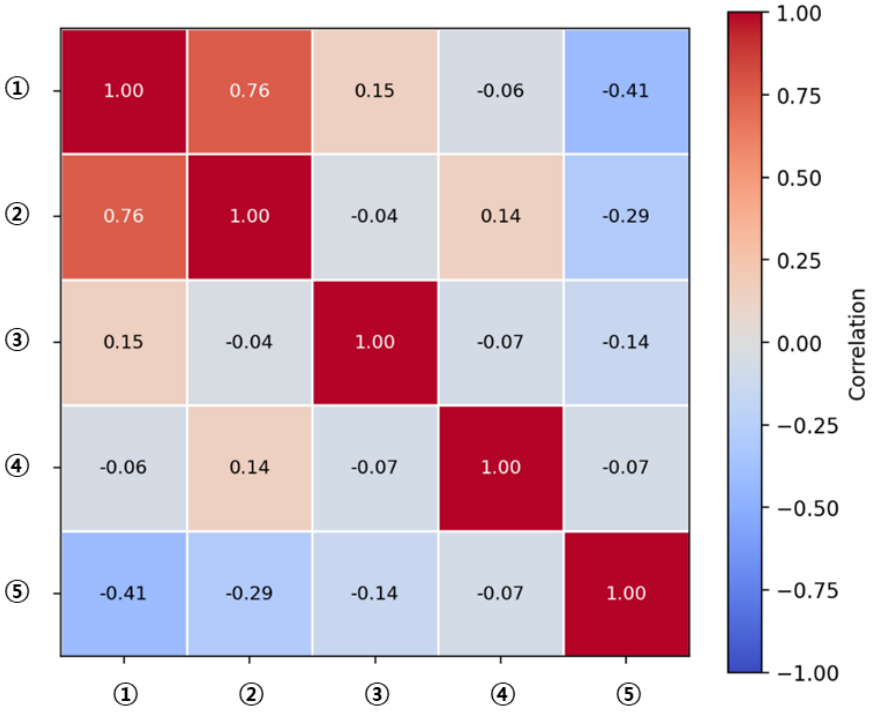

b

	VIF
①	37.2
②	53.9
③	14.7
④	24.4
⑤	43

Fig. S20. (a) Correlation heatmap and (b) variance inflation factor for the 5 features.

Table S1. Equivalent circuit fitting parameters for the LFP cathode measured in a three-electrode full-cell at 0 and 10 cycles.

	R_s (Ω)	R_{ct} (Ω)	R_d (Ω)
0 cyc.	1.15	2.30	4.01
10 cyc.	1.23	1.81	2.90

Table S2. Key design parameters for 79 different cells.

Cell #	Current density	Cathode			Anode			Electrolyte	Formation cut-off voltage
		Material	L/L	L/D	Material	L/L	L/D		
#1	h	b+c	i	b	b	o	g	b	3.8V
#2	h	b+c	i	b	b	o	g	b	3.8V
#3	i	b+c+LFO 2%	j	b	b	o	g	b	4.2V
#4	i	b+c+LFO 2%	j	b	b	o	g	b	4.2V
#5	i	b+c+LFO 2%	j	b	b	o	i	b	4.2V
#6	i	b+c+LFO 2%	j	b	b	o	i	b	4.2V
#7	i	b+c+LFO 2%	j	b	b	o	j	b	4.2V
#8	i	b+c+LFO 2%	j	b	b	o	j	b	4.2V
#9	c	b+c	d	c	b	g	g	b	3.8V
#10	c	b+c	d	c	b	g	g	b	3.8V
#11	b	b+c	d	c	b+Si 2%	b	g	b	3.8V
#12	b	b+c	d	c	b+Si 2%	b	g	b	3.8V
#13	b	b+c+LFO 2%	c	c	b+Si 2%	b	g	b	4.2V
#14	b	b+c+LFO 2%	c	c	b+Si 2%	b	g	b	4.2V
#15	a	b+c+LFO 2%	c	c	b+Si 4%	a	g	b	4.2V
#16	a	b+c+LFO 2%	c	c	b+Si 4%	a	g	b	4.2V
#17	d	b	f	b	a	g	d	a	3.8V
#18	d	b	f	b	a	g	d	a	3.8V
#19	d	b	f	b	a	h	e	a	3.8V

#20	d	b	f	b	a	h	e	a	3.8V
#21	d	e	f	b	a	m	d	b	3.8V
#22	d	e	f	b	a	m	d	b	3.8V
#23	d	e	f	b	a	g	d	b	3.8V
#24	d	e	f	b	a	g	d	b	3.8V
#25	d	e	f	b	c	f	d	b	3.8V
#26	d	e	f	b	c	f	d	b	3.8V
#27	d	a	f	b	a	g	d	b	3.8V
#28	d	a	f	b	a	g	d	b	3.8V
#29	e	b+c	d	b	b	j	h	b	3.8V
#30	e	b+c	d	b	b	j	h	b	3.8V
#31	e	b+c	d	b	b	j	h	c	3.8V
#32	e	b+c	d	b	b	j	h	c	3.8V
#33	c	b+c	a	a	b	d	f	b	3.8V
#34	c	b+c	a	a	b	d	f	b	3.8V
#35	c	b+c	a	a	b	d	f	c	3.8V
#36	c	b+c	a	a	b	d	f	c	3.8V
#37	c	b	a	a	b	c	f	b	3.8V
#38	c	b	a	a	b	c	f	b	3.8V
#39	c	b	a	a	b	c	f	c	3.8V
#40	c	b	a	a	b	c	f	c	3.8V
#41	f	a+c	g	b	b	l	f	b	3.8V
#42	f	a+c	g	b	b	l	f	b	3.8V
#43	f	a+c	g	b	b	l	f	b	3.8V

#44	f	a+c	g	b	b	l	f	b	3.8V
#45	f	a+c	g	b	b	l	f	b	3.8V
#46	f	b+c	g	b	b	l	f	b	3.8V
#47	f	b+c	g	b	b	l	f	b	3.8V
#48	f	b+c	g	b	b	l	f	b	3.8V
#49	f	a+c	g	b	b	l	f	b	3.8V
#50	f	a+c	g	b	b	l	f	b	3.8V
#51	f	a+c	g	b	b	l	f	b	3.8V
#52	f	a+c	g	b	b	l	f	b	3.8V
#53	e	b+c+LFO 2%	e	b	b	i	f	b	3.65V
#54	e	b+c+LFO 2%	e	b	b	i	f	b	3.65V
#55	e	b+c+LFO 2%	e	b	b	i	f	b	4.2V
#56	e	b+c+LFO 2%	e	b	b	i	f	b	4.2V
#57	e	a+c+LFO 2%	b	b	b	i	f	b	3.65V
#58	e	a+c+LFO 2%	b	b	b	i	f	b	3.65V
#59	e	a+c+LFO 2%	b	b	b	i	f	b	4.2V
#60	e	a+c+LFO 2%	b	b	b	i	f	b	4.2V
#61	e	b+c	d	b	b	k	f	b	3.8V
#62	e	b+c	d	b	b	k	f	b	3.8V
#63	e	b+c	d	b	b	e	b	b	3.8V
#64	e	b+c	d	b	b	e	b	b	3.8V
#65	e	b+d	d	b	b	k	f	b	3.8V
#66	e	b+d	d	b	b	k	f	b	3.8V
#67	e	a+d	d	b	b	k	f	b	3.8V

#68	e	a+d	d	b	b	k	f	b	3.8V
#69	e	b+c	d	b	b	k	f	b	3.8V
#70	e	b+c	d	b	b	k	f	b	3.8V
#71	e	b+c+LFO 2%	e	b	b	i	c	b	4.2V
#72	e	b+c+LFO 2%	e	b	b	i	c	b	4.2V
#73	e	b+c+LFO 2%	e	b	b	i	a	b	4.2V
#74	e	b+c+LFO 2%	e	b	b	i	a	b	4.2V
#75	e	b+c+LFO 2%	e	a	b	i	f	b	4.2V
#76	e	b+c+LFO 2%	e	a	b	i	c	b	4.2V
#77	e	b+c+LFO 2%	e	a	b	i	c	b	4.2V
#78	g	b+c+LFO 2%	h	b	b	n	f	b	4.2V
#79	g	b+c+LFO 2%	h	b	b	n	f	b	4.2V

References

S1. W. M. Dose, C. Xu, C. P. Grey and M. F. L. De Volder, *Cell Rep. Phys. Sci.*, 2020, **1**, 100253.

S2. M. Lewerenz, A. Marongiu, A. Warnecke and D. U. Sauer, *Journal of Power Sources*, 2017, **368**, 57–67.